

MODELING OF PHOTOGENERATED CURRENT IN CIGS GRADED SOLAR CELLS

E. IHALANE*, L. ATOURKI, H. KIROU, A. IHLAL, K. BOUABID

*Laboratoire Matériaux et Energies Renouvelables (LMER), Université Ibn Zohr
Dép. Physique, Faculté des sciences B.P.8106, Hay Dakhla, 80000 Agadir,
Morocco.*

In this paper, an analytical model for the simulation of the photocurrent generated in graded CIGS based solar cells has been developed. The electron-hole pair generation rate and the photo-generated current J_L were determined analytically and then modulated as function of thickness, gap energy and graded acceptor concentration N_A . Based on the simulation results, an optimal graded band-gap structure for the CIGS solar cell has been proposed. The optimum thickness of graded CIGS absorber layer determined by numerical simulation is found to be around 3 μm and the highest J_L is around 34.84 mA/cm^2 . The simulation presented shows how cell parameters can be varied to improve the cell performances.

(Received August 29; Accepted October 16, 2015)

Keywords: Band gap grading; CIGS; Solar cells; Thin films

1. Introduction

Chalcopyrite semiconductors are nowadays the most promising absorber materials in second generation thin film solar cells as they have exhibited conversion efficiencies higher than all their counterpart using silicon, or CdTe. The best Cu(In,Ga)Se₂ (CIGS) laboratory solar cell has reached higher conversion efficiency values, during the last years: the conversion efficiency record was improved by 1.8% from 19.9 in 2008 [1], to 21.7 % in 2014 [2]; 20.3 % in 2010 [3], 20.4% in 2013 [4] and 20.8% in 2014 [5]. Such performances were achieved via the well known co-evaporation process. This is due particularly to their band gap value that can be tailored and adjusted by addition of column III chemical elements to match the solar spectrum. More, further improvements in the CIGS based solar cells are expected. One way to increase the performances of the solar cell relay in the reduction of the recombination of photo-generated electron-hole pairs at the interface between the absorber and the window layers and to facilitate the diffusion of minority carriers in the back contact of the cell. This might be reached by using absorbers with high gap energy near the window layer. The use of tandem CIGS cell or adequate choice of band gap profile of the absorber could fit this request and then improve the performance of solar cell parameters. Indeed, grading or double grading the band gap value of CIGS by addition of Ga element is found to increase the open circuit voltage V_{oc} , photon absorption and carrier diffusion [6-9]. Many profiles of CIGS band gap have been theoretically and numerically studied [10,11].

In CIGS based solar cells the absorber layer is p-type. p-CIGS doping is due to the presence of crystal defects generating acceptor states (intrinsic doping). Indeed, the acceptor level are mainly due to the deficiencies of copper (V_{Cu}) and indium (V_{In}), as well as to the substitutions of copper by indium (Cu_{In}). The beneficial effects of Na on CIGS properties are such that its presence is now considered essential for reaching high efficiencies. The primary improvements are in the open-circuit voltage (V_{oc}) and often in fill factor (FF) with little or no change in collected current [12,13].

*Corresponding author: hassanihalane@gmail.com

Soda lime glass (SLG) substrate, widely used in CIGS cells, contains Na as an oxide (Na_2O). This oxide could be a source of Na. Indeed, molybdenum (Mo) back contacts serve as transport gates for Na diffusion from the SLG into the CIGS absorber layer during high temperature processing [14]. The main effect of Na is that it can limit the formation of donor defects compensatory [15,16]. This can lead to increasing the net density of acceptors N_A and therefore the p-doping [17-19].

In this paper, we report on the analytical calculation of generated photocurrent density J_L in double linearly graded CIGS based solar cells. We have simulated the carrier generation rate as function of thickness and gap energy to prove that it is possible to design a lower band gap and linear doping for current improvement in the same device by appropriate band gap grading.

2. Analytical methodology

2.1. Theoretical model

CIGSe are materials with direct band-gap absorption characterized by an absorption coefficient given by the eq. (1) [20]:

$$\alpha(h\nu, x) = \begin{cases} A\sqrt{h\nu - E_g(x)} & h\nu \geq E_g(x) \\ 0 & h\nu < E_g(x) \end{cases} \quad (1)$$

Where $E_g(x)$ is the band-gap of the material varies with the depth x , $h\nu$ is the photon energy of the incident radiation and $A=5.10^4 \text{cm}^{-1} \text{eV}^{-1/2}$ is a constant which depends upon on the effective masses of electrons and holes in the conduction and valence bands, respectively.

We present one dimensional model for calculating the limiting photocurrent density of the graded band gap solar cell. As shown in Fig.1, We have considered the band gap energy of CIGS with a linear variation of the band-gap from $E_{g,\text{front}}$ to $E_{g,\text{min}}$ in first region, and uniform band-gap $E_{g,\text{min}}$ in the second region, and in the third region it increases linearly from $E_{g,\text{min}}$ to $E_{g,\text{back}}$.

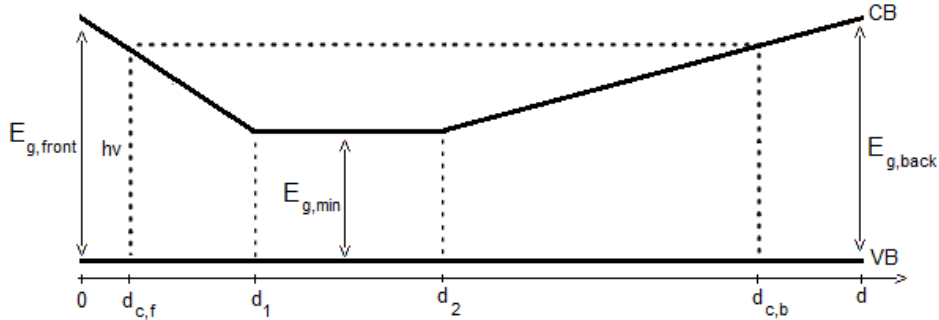


Fig. 1. Energy diagram for a variable-gap CIGS

Graded band gap depends on the depth x , E_g is given as a function of x by eq. (2):

$$E_g(x) = \begin{cases} E_{g,\text{front}} - \beta x & 0 \leq x < d_1 \\ E_{g,\text{min}} & d_1 \leq x < d_2 \\ E'_{g,\text{min}} + \delta x & d_2 \leq x \leq d \end{cases} \quad (2)$$

β and δ are the front grading and back grading parameters given by

$$\beta = \frac{E_{g,\text{front}} - E_{g,\text{min}}}{d_1} \quad (3a)$$

$$\delta = \frac{E_{g,back} - E_{g,min}}{d - d_2} \quad (3b)$$

$$E'_{g,min} = \frac{E_{g,min} \cdot d - E_{g,back} \cdot d_2}{d - d_2} \quad (3c)$$

A photon with energy $h\nu$ between $E_{g,f}$ and $E_{g,min}$ ($E_{g,min} < h\nu < E_{g,back}$) will be absorbed by band to band absorption from the coordinate $d_{c,f}$ is given by expression:

$$d_{c,f} = \left(\frac{E_{g,f} - h\nu}{E_{g,f} - E_{g,m}} \right) d_1 \quad (4)$$

For photon energies ($E_{g,min} < h\nu < E_{g,back}$) will be absorbed by band to band absorption up to the critical distance $d_{c,b}$ is given by Eq. (5).

$$d_{c,b} = \left(\frac{h\nu - E_{g,m}}{E_{g,b} - E_{g,m}} \right) d + \left(\frac{E_{g,b} - h\nu}{E_{g,b} - E_{g,m}} \right) d_2 \quad (5)$$

2.2. Determination of the carrier generation rate

The electron-hole photogenerated rate in the cell as function of photon energy and the depth from cell surface is given by the relation (6) [21], where $N(x, h\nu)$ is the number of photons determined by the absorption coefficient $\alpha(x, h\nu)$ at wavelength λ relative to the number of photons at that wavelength entering the device and x is the position from the semiconductor surface.

$$g(x, h\nu) = -\frac{\partial N(x, h\nu)}{\partial x} = \alpha(x, h\nu) N(x, h\nu) \quad (6)$$

And so $d_{c,f} \leq x < d_1$, the flux $N(x, h\nu)$ solution of Eq. (6) is:

$$N_1(x, h\nu) = N_0 \exp \left\{ -\frac{2A}{3\beta} \left[(h\nu - E_{g,f} + \beta x)^{3/2} - (h\nu - E_{g,f})^{3/2} \right] \right\} \quad (7)$$

Where N_0 is the photon flux density at $x=0$ and where we have neglected the surface reflection. The spectrum used in these calculations is an AM 1.5 spectrum.

The hole-electron pair generation rate $g_1(x, h\nu)$ at depth x ($x > d_{c,f}$) given by Eq. (8), and from $x=0$ to $d_{c,f}$ is $g_1 = 0$.

$$g_1(x, h\nu) = N_0 A (h\nu - E_{g,f} + \beta x)^{1/2} \exp \left\{ -\frac{2A}{3\beta} \left[(h\nu - E_{g,f} + \beta x)^{3/2} - (h\nu - E_{g,f})^{3/2} \right] \right\} \quad (8)$$

For $d_1 \leq x < d_2$, the useful photon flux incident on region 2 is given by

$$N_2(x, h\nu) = N_2(d_1, h\nu) \cdot \exp \left\{ -A (h\nu - E_{g,m})^{1/2} (x - d_1) \right\} \quad (9)$$

Where for our model cell, $g_2(x, h\nu)$ is given by Eq. (11) and the boundary conditions are

$$N_2(x, h\nu) = N_1(x, h\nu) \quad \text{at } x = d_1 \quad (10a)$$

$$N_2(d_1, h\nu) = N_0 \cdot \exp\left\{-\frac{2A}{3\beta} \left[(h\nu - E_{g,f} + \beta d_1)^{3/2} - (h\nu - E_{g,f})^{3/2} \right]\right\} \quad (10b)$$

$$g_2(x, h\nu) = N_2(d_1, h\nu) \cdot A(h\nu - E_{g,m})^{1/2} \exp\left\{-A(h\nu - E_{g,m})^{1/2}(x - d_1)\right\} \quad (11)$$

For $d_2 \leq x \leq d_{c,b}$, the flux at a depth x is given by

$$N_3(x, h\nu) = N_3(d_2, h\nu) \cdot \exp\left\{\frac{2A}{3\delta} \left[(h\nu - E'_{g,m} - \delta x)^{3/2} - (h\nu - E'_{g,m} - \delta d_2)^{3/2} \right]\right\} \quad (12)$$

The boundary conditions are

$$N_3(x, h\nu) = N_2(x, h\nu) \quad \text{at } x = d_2 \quad (13a)$$

$$N_3(d_2, h\nu) = N_0 \cdot \exp\left\{-\frac{2A}{3\beta} \left[(h\nu - E_{g,f} + \beta d_1)^{3/2} - (h\nu - E_{g,f})^{3/2} \right] - [A(h\nu - E_{g,m})^{1/2}(d_2 - d_1)]\right\} \quad (13b)$$

The term g_3 is the generation rate of carriers in region 3, given by:

$$g_3(x, h\nu) = N_3(d_2, h\nu) \cdot A(h\nu - E'_{g,m} - \delta x)^{1/2} \exp\left\{\frac{2A}{3\delta} \left[(h\nu - E'_{g,m} - \delta x)^{3/2} - (h\nu - E'_{g,m} - \delta d_2)^{3/2} \right]\right\} \quad (14)$$

The carrier collection can be significantly improved with the additional electrical field obtained from Ga-grading and doping grading. The collection probability defined in Eq. (15) [22].

$$f_c(x) = \exp(\xi x/2) \times \frac{\cosh[(W-x)/L'_n] + (S'_n L'_n / D_n) \sinh[(W-x)/L'_n]}{\cosh(W/L'_n) + (S'_n L'_n / D_n) \sinh(W/L'_n)} \quad (15)$$

$$\text{Where} \quad S'_n = S_n + \xi D_n / 2 \quad \text{and} \quad L'_n = L_n / \sqrt{1 + (\xi L_n / 2)^2}$$

where L'_n the effective minority carrier diffusion length, S'_n the effective recombination velocity at the back contact, W the width of the region considered, D_n the diffusion constant and d the CIGS layer thickness.

In the space charge region (region1), all photons absorbed in the SCR must contribute to the photocurrent as a result of high electrical field. So $f_c(x)$ in SCR can be expressed as [23]

$$f_c(x) = 1 \quad d_{c,f} \leq x < d_1 \quad (16)$$

The resultant electric field in the region 3 is given by [22]

$$\xi = \frac{\partial}{\partial x} [\ln(N_A(x))] + \frac{1}{kT} \frac{\partial E_g}{\partial x} \quad (17)$$

Where k is the Boltzmann constant and T is the absolute temperature. The case that $N_A(x)$ is uniform ($\partial[\ln(N_A(x))]/\partial x = 0$), for the case that $N_A(x)$ is a parabolic function of x is given by equation Eq. (18), for the case that $N_A(x)$ is a linear function of x expressed by Eq. (19), the

acceptor concentration maximal $N_{A,max}$ and minimal $N_{A,min}$ in the region 3 were assumed to 10^{16} and 10^{17} cm^{-3} , respectively.

$$N_A(x) = N_{A,min} + \left(\frac{N_{A,max} - N_{A,min}}{(d - d_2)^2} \right) \cdot (x - d_2)^2 \quad (18)$$

$$N_A(x) = N_{A,min} + \left(\frac{N_{A,max} - N_{A,min}}{(d - d_2)} \right) \cdot (x - d_2) \quad (19)$$

Every term of the illumination current density is calculated from this equation: [24,25]

$$J_{L,i} = q \int d(h\nu) \int g_i(x, h\nu) f_{c,i}(x) dx \quad (20)$$

The total current density of the cell is:

$$J_L = \sum_{i=1}^3 J_{L,i} \quad (21)$$

3. Modulation results for graded CIGS solar cell

3.1. Effect of the thickness $d_2 - d_1$ and $E_{g,back}$

Fig. 2 shows J_L as function of thickness $d_2 - d_1$ and $E_{g,back}$. As expected, J_L decreased steadily with increasing $d_2 - d_1$. For example, J_L decreased from 33 to 30.75 mA/cm^2 for $d_2 - d_1 = 0$ and $d_2 - d_1 = 0.5 \mu\text{m}$. However, as $E_{g,back}$ continued to increase, J_L soon reached a maximum and then started to decrease, reached a maximum for $E_{g,back}$ in the range $1.3 \leq E_{g,back} \leq 1.55$ and the highest value is 33.22 for $E_{g,back} = 1.4 \text{eV}$. Band gap minimal ($E_{g,min}$) and the thickness of space charge region (d_1) were chosen to be 1.1 eV and $0.3 \mu\text{m}$, respectively.

In the following of this work, we have used as values of thickness $d_2 - d_1$ and $E_{g,back}$ are 0 and 1.4 eV, respectively.

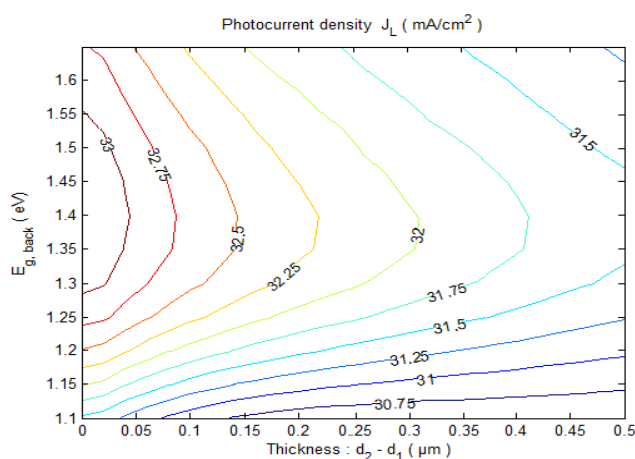


Fig. 2 Calculated photocurrent density J_L as a function of thickness $d_2 - d_1$ and back bandgap $E_{g,back}$ assuming $E_{g,front} = 1.3 \text{eV}$, $E_{g,min} = 1.1 \text{eV}$ and $L_n = d_1 = 0.3 \mu\text{m}$.

3.2. Effect of the front bandgap $E_{g,front}$

As seen in Fig. 3 the light absorbed in the SCR layer improves the cell parameters significantly only if the cell band-gap front is small. It can be seen that the improvement in J_L

decreases when the value of front bandgap is increased. The decrease in J_L is more significant in the case of $d = 1\mu\text{m}$, since the photocurrent density is more important for $3\mu\text{m}$ thickness.

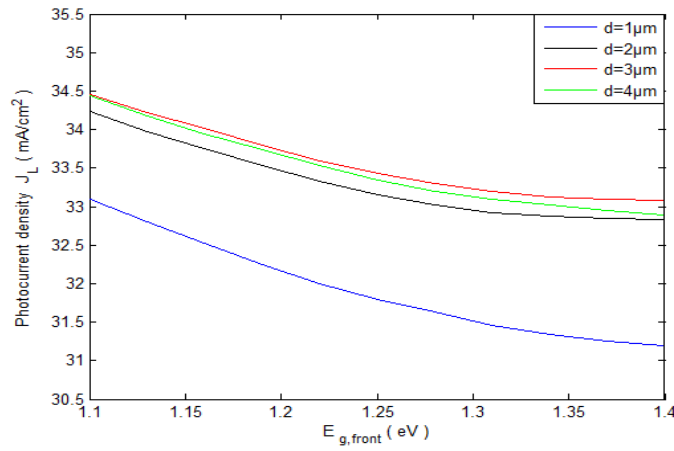


Fig. 3. Variation of the J_L versus front bandgap, assuming $E_{g,back}=1.4\text{eV}$, $E_{g,min}=1.1\text{eV}$ and $L_n=d_l=0.3\mu\text{m}$

3.3. Effect of the graded acceptor concentration N_A

In the following, we present the results of the calculation of the photocurrent density J_L as function of thickness (d) for uniform, parabolic and linear repartition of acceptor element N_A (Fig. 4). As we can see, the photocurrent increases with thickness and it reaches a maximum value for thickness upper than $3\mu\text{m}$. The best photocurrent densities value (34.84 mA/cm^2) is given by linear distribution of acceptor concentration.

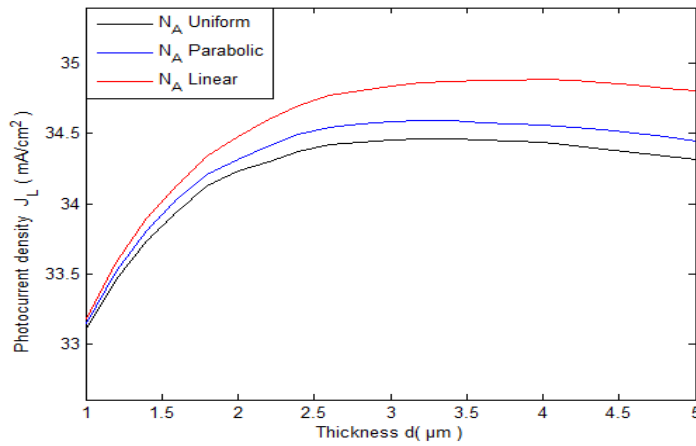


Fig. 4. Variation of the photo-current J_L versus the solar cell thickness for different N_A repartition, assuming $E_{g,front}=E_{g,min}=1.1\text{eV}$ and $L_n=d_l=0.3\mu\text{m}$

To explain the rise of the photocurrent density, comparing with the other two doping profiles, we consider in the region 3 ($d_2 \leq x \leq d$) the distribution of N_A in CIGS (Fig. 1) is divided into N small zone and the length of each zone is $(d-d_2)/N$, incremental numbered from left to the right (Fig. 5).

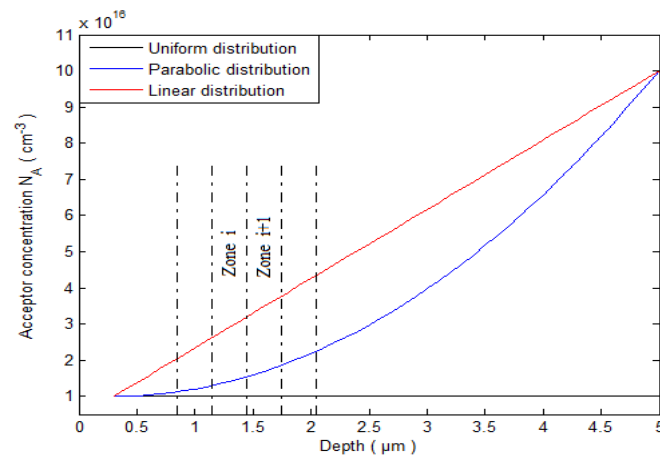


Fig. 5. Distribution of acceptor concentration N_A in CIGS

The zone numbered $i+1$ is more heavily doped than the zone i for the linear profile than the other ones, this leads to create a potential barrier. The potential barrier induced by the doping level of the difference between the two zones tends to confine the minority carriers in i -zone, the same process occurs between each adjacent two zones, so the electrons move toward the space charge region. In most of the region 3, in particular the proximal portion of SCR, the doping level difference between two adjacent zones is more important in case of linear doping compared to uniform and parabolic profiles.

4. Conclusion

In this work, we have developed an analytical model to calculate the photocurrent of linearly graded CIGS based solar cell. In this model, the absorber layer thickness is divided on three regions. For each region, we formulate the photo-generated current which includes the contribution of the generation rate. The total photocurrent density is assumed to be the sum of the photocurrent density over the all regions. It is found that J_L depends on the profile of the doping layer.

References

- [1] L Repin, AM. Contreras, B. Egaas, C. Dehart, 1. Scharf, c.L. Perkins, B. To, R. Noufi, Prog. Photovolt. Res. Appl. **16**, 235 (2008).
- [2] Philip Jackson, Dimitrios Hariskos, Roland Wuerz, Oliver Kiowski, Andreas Bauer, Theresa Magorian Friedlmeier, Michael Powalla, Phys. Status Solidi RRL, 1-4 (2014).
- [3] P. Jackson, D. Hariskos, E. Lotter, S. Paetel, R. Wuerz, R. Menner, W. Wischmann, M. Powalla Prog. Photovolt. Res. Appl. **19**, 894 (2011).
- [4] Adrian Chirila, Patrick Reinhard, Fabian Pianezzi, Patrick Bloesch, Alexander R. Uhl, Carolin Fella, Lukas Kranz, Debora Keller, Christina Gretener, Harald Hagendorfer, Dominik Jaeger, Rolf Erni, Shiro Nishiwaki, Stephan Buecheler and Ayodhya N. Tiwari, Nature Materials **12**, 1107 (2013).
- [5] Philip Jackson, Dimitrios Hariskos, Roland Wuerz, Wiltraud Wischmann, Michael Powalla, Phys. Status Solidi RRL **8**(3), 219 (2014).
- [6] O. Lundberg, M. Edoff, L. Stolt, Thin Solid Films **480–481**, 520 (2005).
- [7] Darius Kuciauskas, Jian V. Li, Miguel A. Contreras, Joel Pankow, Patricia Dippo, Matthew Young, Lorelle M. Mansfield, Rommel Noufi, and Dean Levi, Charge, Journal of Applied Physics **114**, 154505 (2013).

- [8] J. Song, S. S. Li, C.H. Huang, O.D. Crisalle, T.J. Anderson, *Solid-State Electronics* **48**, 73 (2004).
- [9] T. Dullweber, G. Hanna, U. Rau, H.W. Schock, *Solar Energy Materials & Solar Cells* **67**, 145 (2001).
- [10] M. Gloeckler, J.R. Sites, *Journal of Physics and Chemistry of Solids* **66**, 1891 (2005).
- [11] T. Dullweber, G. Hanna, W. Shams-Kolahi, A. Schwartzlander, M.A. Contreras, R. Noufi, H.W. Schock, *Thin Solid Films* **361-362**, 478 (2000).
- [12] Pedro Salomé, Viktor Fjallstrom, Adam Hultqvist, and Marika Edoff, *IEEE JOURNAL OF PHOTOVOLTAICS*, **3**(1), 509 (2013).
- [13] A. Rockett, *Thin Solid Films* **480-481**, 2 (2005).
- [14] A. Rockett, K. Granath, S. Asher, M.M. Al Jassim, F. Hasoon, R. Matson, B. Basol, V. Kapur, J.S. Britt, T. Gillespie, C. Marshall, *Solar Energy Materials & Solar Cells* **59**, 255 (1999).
- [15] Miguel A. Contreras, B. Egaas, P. Dippo, J. Webb, J. Granata, K. Ramanathan, S. Asher, A. Swartzlander, and R. Noufi, On The Role Of Na And Modifications To Cu(Ln,Ga)Se, Absorber Materials Using Thin-Mf: (M=Na, K, Cs) Precursor Layers, 26th IEEE PVSC, 359 – 362 (1997).
- [16] David J. Schroeder and Angus A. Rockett, *Journal of Applied Physics* **82**, 4982 (1997).
- [17] Tokio Nakada, *Electronic Materials Letters*, **8**(2), 179 (2012).
- [18] D. Braunger, D. Hariskos, G. Bilger, U. Rau, H.W. Schock, *Thin Solid Films* **361-362**, 161 (2000).
- [19] Tokio Nakada, Hiroki Ohbo, Masakazu Fukuda, Akio Kunioka, *Solar Energy Materials and Solar Cells* **49**, 261 (1997).
- [20] N.H. Rafat, A.M. Abdel Haleem, S.E.-D. Habib, *Renewable Energy* **32**, 21 (2007).
- [21] J. Mattheis, P.J. Rostan, U. Rau, J.H. Werner, *Solar Energy Materials & Solar Cells* **91**, 689 (2007).
- [22] Martin A. Green, *Prog. Photovolt: Res. Applications* **17**, 57 (2009).
- [23] Kanglin Xiong, Shulong Lu, Taofei Zhou, Desheng Jiang, Rongxin Wang, Kai Qiu, Jianrong Dong, Hui Yang, *Solar Energy* **84**, 1888 (2010).
- [24] Arturo Morales-Acevedo, *Solar Energy Materials & Solar Cells* **95**, 2837 (2011).
- [25] Nima E. Gorji, Ugo Reggiani, Leonardo Sandrolini, *Solar Energy* **86**, 920 (2012).